The Role of the Unfolded State in Hairpin Stability

Hongxing Lei and Paul E. Smith
Department of Biochemistry, Kansas State University, Manhattan, Kansas 66506-3702

ABSTRACT The effects of a T3S mutation on the stability of a 3:5 β-hairpin forming peptide (YITNSNGTWT) are investigated. Molecular dynamics simulations in explicit water indicate that the wild-type peptide forms a stable hairpin whereas the T3S mutant does not, in agreement with the experimental data. Thermodynamic integration calculations for the mutation of Thr to Ser suggest that the free-energy changes in the folded state are small, but the corresponding changes in the unfolded state are large and favorable. One of the main reasons for the difference appears to be the formation of a stable cluster involving the Tyr1 and Ser3 hydroxyl groups and their interaction with the C-terminal carboxylate group, which was observed after unfolding of the T3S mutant. Further analysis of the side-chain preferences of Thr and Ser indicate that the corresponding cluster in the wild-type peptide is unstable due to the high preference of the Thr χ^1 dihedral for g^+ states, which appeared to be incompatible with formation of a stable cluster. The results suggest that one should consider the nature of the unfolded state when attempting to fully explain the effects of mutations on hairpin stability.

INTRODUCTION

A complete understanding of the formation and stability of protein secondary structural elements will provide valuable insights into the early stages of protein folding (Baldwin and Rose, 1999; Brooks, 2002). One such element is the β-hairpin, a proposed precursor in β-sheet formation. Nuclear magnetic resonance (NMR) studies of hairpins and their mutants have demonstrated that side-chain contacts (Ramirez-Alvarado et al., 1996; Syud et al., 2001), side-chain packing (de Alba et al., 1997b), side-chain hydrogen bonding (de Alba et al., 1997a), turn sequence preference (de Alba et al., 1997a, 1999; Santiveri et al., 2000; Munoz et al., 1997), and salt bridge formation (Ramirez-Alvarado et al., 2001; Zerella et al., 2000) may all be important for hairpin formation. Computer simulations of hairpin folding and unfolding have also been used to help elucidate the atomic level interactions responsible for hairpin stability (Daura et al., 2001; Ma and Nussinov, 2000; Zhou et al., 2001; Klimov et al., 2002; Schaefer et al., 1998; Ferrara et al., 2002). However, in attempting to explain the formation and stability of different hairpins, the vast majority of the experimental and theoretical studies have focused almost exclusively on changes in the interactions within the native state conformation.

A good example of a small hairpin forming peptide has been described by de Alba et al. They designed a 10-residue peptide (P5: YITNSDGTWT), derived from fragment 15–23 of tendamistat, which has been characterized as having a high propensity for a single 3:5 β-hairpin structure (de Alba et al., 1997b). Residues 1–4 and 8–10 form the strand residues, whereas residues 5–7 constitute the turn (see Fig. 1). The peptide folds to form a single 3:5 β-hairpin structure with an 80% population in water at 275 K, as estimated from nuclear Overhauser enhancement (NOE) signals. A T3S mutant of P5 was also studied and shown to adopt the same 3:5 β-hairpin in solution, but with a lower population of 20%. Considering a simple two-state equilibrium between folded and unfolded peptide, the above populations correspond to folding free energies of -3.5 kJ/mol for the wild-type (WT) and 3.5 kJ/mol for the T3S mutant, a difference of -7 kJ/mol in favor of the unfolded form of the T3S mutant. This represents a sizeable change in stability in comparison with the relatively small difference in amino acid structure of just one methyl group.

Our previous computer simulations of a neutral version of P5 (YITNSNGTWT) using the GROMOS (43a1) force field have demonstrated that hairpin formation can be observed in explicit solvent within 20 ns under normal conditions (300 K, 1 atm) and without the need for enhanced sampling techniques (unpublished data). The final stable 3:5 hairpin structure is shown in Fig. 1 and was in good agreement with the NOE-derived interproton distances. Furthermore, other 2:2 and 4:4 hairpins were not stable, suggesting that the GROMOS force field provides a reasonable description of the interactions within this system. The side chain of Thr3 forms a close contact with the side chain of Trp9 in the folded state. However, examination of the simulation data indicates that removal of the Thr methyl group would result in a decrease of -0.1 nm^2 in the hydrophobic solvent accessible surface area of the native state. The corresponding change in the unfolded state is unknown but cannot be much larger than the difference in surface area of the two isolated amino acids, which is approximately -0.25 nm^2 (Creighton, 1984). Using a microscopic surface tension value of 10 kJ/mol/nm^2 (Creighton, 1984), the above surface-area changes for mutation of Thr3 to Ser predict that the native state is stabilized by -1.0 kJ/mol and the unfolded state by -2.5 kJ/mol. The overall change of -1.5 kJ/mol in favor of the unfolded state for the T3S mutant is considerably less than the experimental estimate of -7 kJ/mol (de Alba et al.,

Submitted June 18, 2003, and accepted for publication July 25, 2003.

Address reprint requests to Paul E. Smith, Dept. of Biochemistry, 36 Willard Hall, Kansas State University, Manhattan, KS 66506-3702. Tel.: 785-532-5109; Fax: 785-532-7278; E-mail: pesmith@ksu.edu.

0006-3495/03/12/3513/08 $2.00

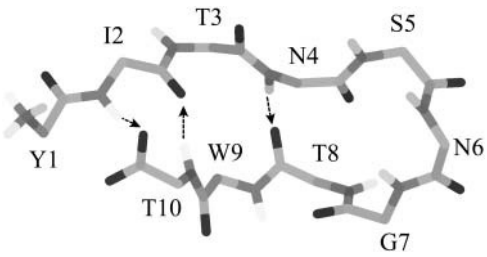

FIGURE 1 The 3:5 hairpin structure adopted by the WT peptide (YITNSNGTWT) as described by the GROMOS force field. Residues 1–4 and 8–10 form part of the strand with residues 5–7 adopting a turn arrangement. Three main-chain hydrogen bonds are located between residues 2→10, 10→2 and 4→8. Only the backbone atoms are shown for clarity.

1997b). Consideration of the differences in the intrinsic free energy for sheet formation between Thr and Ser suggests these contributions are also too small (−1.9 kJ/mol) (Stapley and Doig, 1997) to explain the observed changes.

Recent experimental and theoretical data has indicated that the denatured or unfolded state of peptides and proteins may not be as random as originally thought (Dill and Shortle, 1991; Shortle 1993; O'Connell et al., 1999; Hammack et al., 2001). If so, it becomes just as important to understand the effects of mutations on any favorable or unfavorable interactions present in the unfolded state. Many studies are beginning to probe the properties of unfolded peptide chains (Wilson et al., 1996; Hennig et al., 1999; Fersht and Daggett, 2002; Daura et al., 2002). However, these studies have provided very little atomic level detail of real unfolded structures, especially hairpins, and therefore it is still not clear exactly when one has to consider possible changes in the unfolded state. Consequently, it is important to identify and characterize any possible residual structure present in the denatured or unfolded states of peptides and proteins. In this study we use computer simulations to investigate the differences between the WT and T3S peptides, and quantify these differences using thermodynamic integration (TI) calculations. The results suggest that changes in the unfolded state are more significant (larger) than changes in the native state, and that a detailed knowledge of the unfolded state is therefore essential for a complete understanding of the behavior of the T3S mutant and the thermodynamics of folding.

METHODS

All molecular dynamics simulations were performed using the GROMOS96 program and the 43a1 force field (Scott et al., 1999). The SPC water model (Berendsen et al., 1981) and a truncated octahedron were used for the simulations. The time-step was 2 fs and SHAKE (Ryckaert et al., 1977) was used to constrain all bond lengths with a tolerance of 10^{-4} nm. A twin range cut-off of 0.8 nm/1.4 nm was employed and the nonbonded pair list was updated every 10 steps. Long-range electrostatics were treated using a reaction field approach (Tironi et al., 1995) with a reaction field permittivity for SPC water of 54 (Smith and van Gunsteren, 1994). The simulations were performed under conditions of constant temperature (300 K) and constant pressure (1 atm) using the weak coupling approach (van Gunsteren and Berendsen, 1990). The WT (YITNSNGTWT) and T3S (YISNSNGTWT) peptides were simulated in a box of 1016 water molecules. The starting structure for the T3S simulation was the folded structure formed after 20 ns of the WT simulation described previously (unpublished results). In both the WT and the T3S mutant, the only charged side-chain residue (Asp6) was mutated to Asn to make the peptides neutral. This is a very conservative mutation as both residues are similar in size and shape, and NG and DG display the highest two turn propensities among all XG turns in known protein structures (Griffiths-Jones et al., 1999). The Thr and Ser dipeptide simulations were performed using 450 water molecules for a total of 10 ns each. Errors ($\pm 1\ \sigma$) in populations were estimated from four 2.5-ns averages.

The potential of mean force (pmf) between the C_3^α and C_9^α atoms was determined by umbrella sampling (McCammon and Harvey, 1988) using a harmonic distance restraining potential with a force constant of 10,000 kJ/mol/nm^2. A series of runs were performed differing only in the position of the reference distance, which varied from 0.35 nm to 1.00 nm in increments of 0.05 nm. Probability distributions corresponding to the carbon to carbon distance were then obtained from 250 ps of simulation performed in each window. After correcting the data for the presence of the biasing function, the resulting set of histograms were combined to generate the final pmf using the weighted histogram analysis method (WHAM) approach (Kumar et al., 1992).

Thermodynamic integration calculations were used to determine the change in free energy on mutation of Thr into Ser and vice versa (Kollman, 1993). Mutation of Thr to Ser involved conversion of the neutral united atom methyl group into a dummy atom with the same mass without changing any of the bond, angle, or dihedral energy terms. TI calculations were performed using 11 equally spaced λ values between 0 and 1 with 200 ps of sampling at each λ point after 10 ps of equilibration. The Hamiltonians for the initial and final states were coupled using the soft core approach to avoid possible singularity problems (Beutler et al., 1994) with an α value of 0.5 nm^2 for the van der Waals term. A plot of the free-energy derivatives against λ was subsequently splined to generate 1000 points, and then integrated using a simple trapezoidal integration scheme. Errors ($\pm 1\ \sigma$) were estimated from two or three subaverages.

Additional TI calculations were performed to determine the free-energy change associated with the mutation of Thr to Ser, while maintaining the same ψ and χ^1 rotational states. This was achieved by performing constrained TI calculations using a harmonic dihedral potential ($k = 0.005$ kJ/mol/degree^2) to restrain the main-chain ψ and side-chain χ dihedrals to the appropriate region of dihedral space ($\psi_0 = 120°$ and ${\chi_0}^1 = -180°, -60°$, or $+60°$). A weak constraining potential was chosen which only affected the free-energy surface for large deviations (60°) from the corresponding minimum (Straatsma and McCammon, 1989). The small differences in free energy (± 0.3 kJ/mol) associated with the addition of a constraining potential to the Thr and Ser dipeptide Hamiltonians were accounted for by applying statistical mechanical perturbation theory (Zwanzig, 1954) using reference configurations from the unconstrained dipeptide simulations, and the constraining potential as the perturbation.

RESULTS

Unfolding of the T3S mutant

Our first objective was to determine if the T3S mutant is unstable using the GROMOS96 force field. In our previous simulations, a specific set of interactions was observed that appeared to be important for hairpin stability and was also correlated with the folding process. The interactions included three main-chain hydrogen bonds (2→10, 10→2, and 4→8), a hydrogen bond network mediated by the side chain of Asn4

(6→4, 7→4, and 4→10), and a set of three cross-strand side-chain contacts (residues 1–9, 2–10, and 3–9). The time histories for the nine interactions are displayed in Fig. 2 for both the WT and T3S trajectories. Clearly, although the contacts were maintained (or fluctuated slightly) for the WT simulation, they were lost during the simulation of the T3S mutant. The major unfolding event occurred after 7 ns at which point all three main-chain hydrogen bonds were simultaneously lost. Hence, the GROMOS force field is capable of discriminating between the WT and mutant peptides. This observation, and the previously observed successful folding of the WT peptide, provides some degree of confidence in the simulation results.

Potential of mean force calculations

Unfortunately, both simulations were too short to observe reversible folding and therefore obtain the relative populations of the native hairpin and unfolded states. Much longer simulations, or enhanced sampling techniques, are usually required (Daura et al., 1998; Bartels and Karplus, 1997; Mitsutake et al., 2001). In an effort to characterize the equilibrium between folded and unfolded hairpin states, a pmf calculation was performed. As the NOE intensity between the H^{α} atoms of residues Thr3 and Trp9 was used to estimate the hairpin population from the experimental data, the distance between the backbone C^{α} atoms of residues 3 and 9 was chosen to investigate the free-energy profile for unfolding. The results for the WT and T3S mutant are presented in Fig. 3. The pmfs displayed a single minimum at the contact distance with no minima at larger distances where all the main-chain hydrogen bonds would have been broken. The differences between the two pmfs appeared to be minor with only a small apparent stabilization of the T3S form between 0.6 and 0.8 nm. As there were no minima at larger distances, it appeared the pmf did not fully capture the differences in stability very well. The reasons for this are unclear but could include incomplete sampling of the unfolded state, and difficulties attempting to project a multi-dimensional folding surface onto a single coordinate.

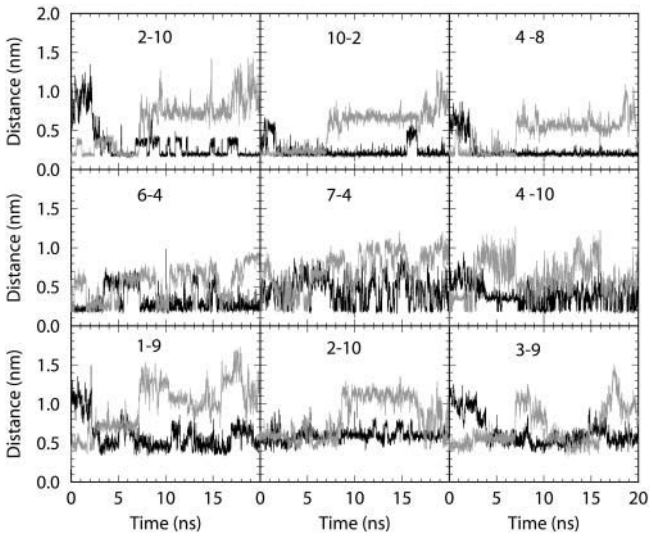

FIGURE 2 Time histories of the nine major contacts defining the folded hairpin. The WT simulation is displayed in black with the T3S simulation in gray. The interactions included three main-chain hydrogen bonds (*top*) corresponding to distances between H_2 and O_{10}, H_{10} and O_2, and H_4 and O_8, three side-chain hydrogen bonds (*middle*) corresponding to distances between O_4^{δ} and H_6, O_4^{δ} and H_7, and N_4^{δ} and O_{10}^{γ}, and three side-chain contacts (*bottom*). The center of mass was used to define the positions of the side chains.

Properties of the Thr and Ser dipeptides

In attempting to explain the effects of the Thr to Ser mutation it will prove useful to characterize the properties of the corresponding blocked single amino acids (N-acetyl, N′-methylamide), or dipeptides, as described by the GROMOS force field. The intrinsic rotamer populations (P) of Thr and Ser were determined from the corresponding dipeptide simulations. The results are displayed in Table 1. The ψ and χ^1 dihedrals underwent multiple (>10) transitions during the simulations, indicating that their populations should be representative, whereas the φ dihedral remained in the $\varphi <$ 0 region for the majority of the trajectory. Both the Thr and Ser dipeptides favored the β state with free-energy differences of $G_{\beta} - G_{\alpha} = -\mathrm{RT} \ln (P_{\beta}/P_{\alpha}) = -4.5$ kJ/mol for Thr and −3.6 kJ/mol for Ser. The difference of −0.9 kJ/mol is in agreement with the estimated relative sheet forming abilities (−1.9 kJ/mol) of the two amino acids (Stapley and Doig, 1997), albeit smaller in magnitude. The χ^1 probability distributions as a function of backbone conformation (α or β) are displayed in Fig. 4. The Thr dipeptide preferred g^+ side-chain conformations with little population of the t state

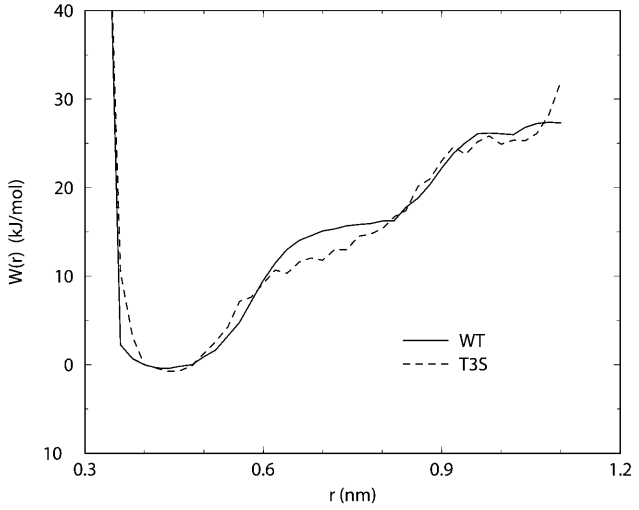

FIGURE 3 The distance-dependent potential of mean force corresponding to the C_3^{α} and C_9^{α} atoms in the WT (*solid*) and T3S (*dashed*) peptides.

TABLE 1 Dihedral distributions from the Thr and Ser dipeptide simulations

			Thr		Ser	
Dihedral	Main chain*	Side chain†	Population (%)	ΔG (kJ/mol)	Population (%)	ΔG (kJ/mol)
ψ	α	−60	14	4.5	19	3.6
	β	+120	86	0	81	0
χ^1	All	−60	15	4.2	44	0
		+60	82	0	18	2.2
		180	3	8.3	42	0.1
χ^1	α	−60	9	5.8	25	1.5
		+60	91	0	46	0
		180	0		29	1.2
χ^1	β	−60	16	4.1 (1)	49	0
		+60	81	0	10	4.0(4)
		180	3	8 (2)	41	0.4(2)

*The α state is defined as $-120° < \psi < +30°$ and the β state refers to any other ψ conformations.
†The g^+, g^-, and t states are defined as having χ^1 values of $+60 \pm 60°$, $-60 \pm 60°$, and $180 \pm 60°$, respectively.
Values in parentheses correspond to estimated errors.

for both α and β backbone arrangements (presumably due to interactions between C^γ and the backbone N and C atoms). On the other hand, all the Ser χ^1 minima (g^-, g^+, and t) were significantly populated. However, the g^+ minima for χ^1 displayed a relatively low population when the backbone was in the highly populated β state conformation.

The free-energy difference for mutation of Thr to Ser was determined by TI calculations (see Table 2). The free energy for mutating Thr to Ser in the dipeptide model system was -2.7 ± 0.5 kJ/mol. In our later discussion it will be useful to refer to the free-energy differences corresponding to the Thr g^+ to Ser g^+, Thr g^- to Ser g^-, and Thr t to Ser t transitions. Hence, additional constrained TI calculations were performed to determine the free-energy change associated with the above transitions when the backbone adopted the highly populated β state (Straatsma and McCammon, 1989). The free-energy difference for mutating Thr in the g^+ state to Ser in the g^+ state was 0.7 kJ/mol, compared to −6.0 and −8.4 kJ/mol for the corresponding g^- and t transitions, respectively. These values, in combination with the populations presented in Table 1, enabled the construction of the free-energy diagram presented in Fig. 5 for the Thr and Ser dipeptides. In constructing the free-energy diagram the TI results were considered to be the most accurate, followed by the g^+/t ratio in the Thr dipeptide and the g^-/t ratio in the Ser dipeptide, both of which possessed multiple (>10) transitions during the dipeptide simulations. Hence, although the relative free-energy differences in Fig. 5 do not agree exactly with all the differences presented in Table 1, they are consistent within the estimated errors. The free-energy diagram illustrates several features that will be important for later discussions. The free-energy difference between the g^+ states of Thr and Ser was small and favored Thr. In contrast, the difference between the g^- and t states was much larger and favored Ser.

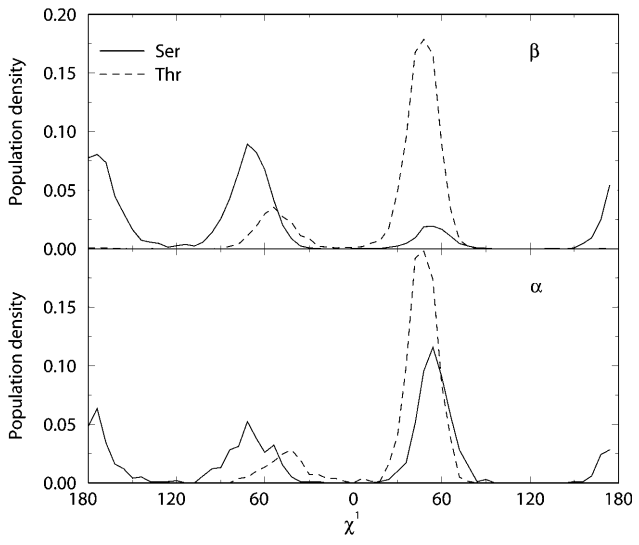

FIGURE 4 Side-chain χ^1 population densities obtained from the Thr and Ser dipeptide simulations. The populations are subdivided according to the main-chain (α or β) conformation.

Thermodynamic integration calculations for the WT and T3S peptides

As it was not possible to reproduce the differences in free energies between the folded and unfolded states using a pmf approach, a series of TI calculations were performed to help quantify changes in the folding thermodynamics. All these calculations were performed without dihedral constraints. The basic approach has been discussed previously (Kollman, 1993) and is outlined in Fig. 6. The difference in folding free energy between the WT and T3S mutant ($\Delta\Delta G$) can be determined by mutating Thr into Ser (or vice versa) in the folded and unfolded states. However, there is a potential complication in this type of approach. Although the folded state is well defined, the unfolded state is unknown and may

TABLE 2 Summary of the TI calculations.

Peptide	Backbone state	Perturbation	ΔG*	$\langle \Delta G \rangle$
T ITN	Random	T→S	−2.7 (5) −2.5 (5)	
WT	Folded	T→S	−1.5 (1); −1.5 (6); 0.6 (1); −4.8 (5); 0.8 (6)	−1.3 (2)
T3S	Unfolded	S→T	9.8 (1); 11.3 (0); 8.2 (6); 3.5 (1)	7.4 (2)
WT	Unfolded	T→S	−7.8 (2); −7.4 (4); −0.9 (4); 0.4 (1); −0.7 (3)	−3.3 (2)

*Free energies are in kJ/mol. Values in parentheses correspond to estimated errors. The values for the WT and T3S mutants correspond to five different initial structures taken from the respective simulations.

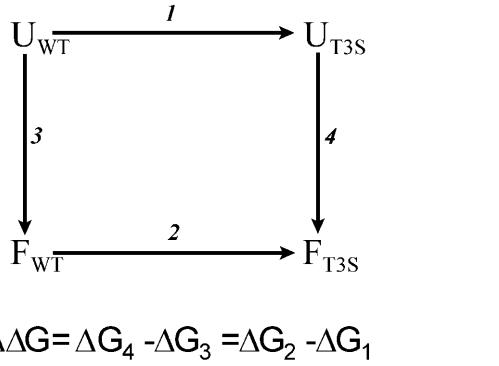

FIGURE 6 An outline of the thermodynamic cycle used to determine changes in the folding thermodynamics. The symbols U and F correspond to the unfolded and folded states, respectively. The NMR data gives $\Delta G_3 = -3.5$ kJ/mol and $\Delta G_4 = 3.5$ kJ/mol, and hence $\Delta\Delta G = 7.0$ kJ/mol. TI calculations were used to determine ΔG_1 and ΔG_2.

be significantly different for the WT and T3S peptides. One approach is to assume an absence of structure in the unfolded state and to perform the corresponding amino acid perturbation for a simple model system (Hu et al., 2003). The simplest model corresponds to a blocked single amino acid residue (dipeptide) which is essentially fully exposed to solvent.

Our initial investigations involved this kind of approach. Table 2 contains the results of a series of TI calculations to determine the free-energy change for mutation of Thr into Ser in the folded and totally random unfolded states. As described previously, the unfolded state modeled by the Thr dipeptide resulted in a ΔG of -2.7 ± 0.5 kJ/mol in favor of Ser. Another TI calculation was performed for the blocked three-amino acid sequence ITN, corresponding to the local sequence in the WT peptide. The ΔG obtained for this system was -2.5 ± 0.5 kJ/mol, which is in agreement with the dipeptide result. Hence, the inclusion of local sequence effects did not appear to change the results. Five different initial folded structures were used to determine the free-energy change for the native hairpin. The average of the five calculations resulted in a ΔG of -1.3 ± 0.2 kJ/mol. These numbers follow the pattern expected from the estimated changes in hydrophobic surface area as discussed in the Introduction (−2.5 kJ/mol for the random state and −1.0 kJ/mol for the folded state). Again, they are too small to explain the experimentally estimated difference.

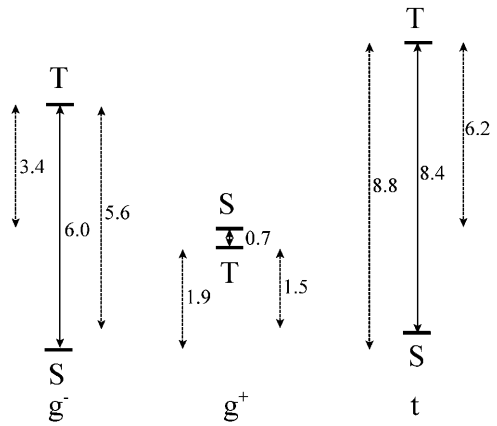

FIGURE 5 Relative free energies (kJ/mol) for the different side-chain conformations of the Thr and Ser dipeptides for the β backbone state. The figure is based on the data from Table 1 and the constrained dihedral TI calculations described in the text. The above free energies result in g^-, g^+, and t side-chain populations of 0.46, 0.16, and 0.38, respectively, for the Ser dipeptide and 0.16, 0.79, and 0.05, respectively, for the Thr dipeptide.

Clearly, the changes in stability did not appear to be due to differences between the WT and T3S forms in the folded state. As we have high confidence in the nature of the folded state, this brings into question our model of the unfolded state. A subsequent set of TI calculations was therefore performed using five different initial structures obtained from the unfolded (>10 ns) section of the T3S mutant trajectory. The average ΔG for the three TI calculations was 7.4 ± 0.2 kJ/mol for the Ser to Thr mutation. The resulting $\Delta\Delta G$ of 6.1 ± 0.3 kJ/mol was in excellent agreement with the difference estimated by NMR (7 kJ/mol). Although the agreement was probably somewhat fortuitous, as both the NMR and simulation data are subject to some error, the results clearly suggest that the major change in hairpin folding thermodynamics was related to significantly larger effects in the unfolded state.

A final set of five TI calculations was then performed using unfolded structures obtained from the early stages of the WT folding simulation. Two of the initial structures displayed very small free-energy differences, similar to that observed for the folded state. However, two of the initial structures generated a large ΔG in favor of Ser, and very similar to the values obtained after using initial structures taken from the T3S unfolded trajectory. Hence, it appeared that the unfolded conformations of the WT peptide may only sample a few of the highly populated conformations corresponding to the T3S mutant, and vice versa. This considerably complicates the determination of free-energy

changes using the TI and thermodynamic cycle approach for small peptides, as one requires the relative population of each distinct conformation in both the initial and final states (Straatsma and McCammon, 1989).

Residual structure in the unfolded state

In an attempt to determine the basis for the increased stability of the unfolded state in the T3S mutant the interactions of the Ser side chain with other amino acid residues were investigated. A stable cluster of interactions was observed shortly after unfolding from the native hairpin. The corresponding time histories are presented in Fig. 7, and a representative configuration is displayed in Fig. 8. The interactions were centered on the C-terminal carboxylate group. There appeared to be a strong affinity of both the Ser and Tyr hydroxyl groups for the carboxylate group. This cluster formed after 8 ns, was then lost after 17 ns, but appeared to be reforming toward the end of the simulation. The C_3^α to C_9^α distance was 0.6 nm when this cluster was intact, suggesting this may be the reason for the small differences observed in the corresponding region of the pmfs shown in Fig. 3. The initial starting structures for the TI calculations were taken from configurations corresponding to 10, 12.5, 15, 17.5, and 20 ns of the T3S trajectory. Hence, the larger ΔG values presented in Table 2 were observed when this interaction was intact (at 10, 12.5, and 15 ns). Analysis of the final structures obtained at $\lambda = 1$ (WT peptide) for these three starting structures indicated that the interaction with the C-terminus was lost. Consequently, the free-energy differences reflected the loss of this interaction.

It was not immediately clear why Thr destabilized the hydroxyl to carboxylate interaction. As discussed earlier, surface area differences between Thr and Ser are too small to explain the observed effect. This leaves two major possibilities, namely, that the introduction of a methyl group interferes with the solvation of the Tyr, Ser, and carboxylate cluster, or that differences in the side-chain rotamer populations are important. To investigate possible solvation effects the three-dimensional water density distribution around the WT and T3S mutant peptides was investigated using a grid-based approach (Makarov et al., 1998) with a grid size of 0.1 nm. On examination of the solvent density, no significant high probability solvation sites were observed in the vicinity of the Thr or Ser side chain (data not shown). Hence, it was concluded that the change in stability did not appear to be a specific solvation effect.

The Ser dipeptide simulation indicated a high preference for the g^- and t arrangements of χ^1. This was in agreement with the distribution of Ser χ^1 values observed during the T3S simulation, which are presented as a time history in Fig. 9. Interestingly, during the time that the cluster of hydroxyl and carboxylate groups was stable (8–17 ns) only

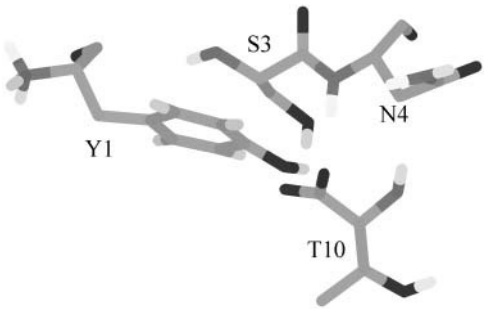

FIGURE 8 A snapshot of the Tyr, Ser, and carboxylate cluster observed during the T3S simulation.

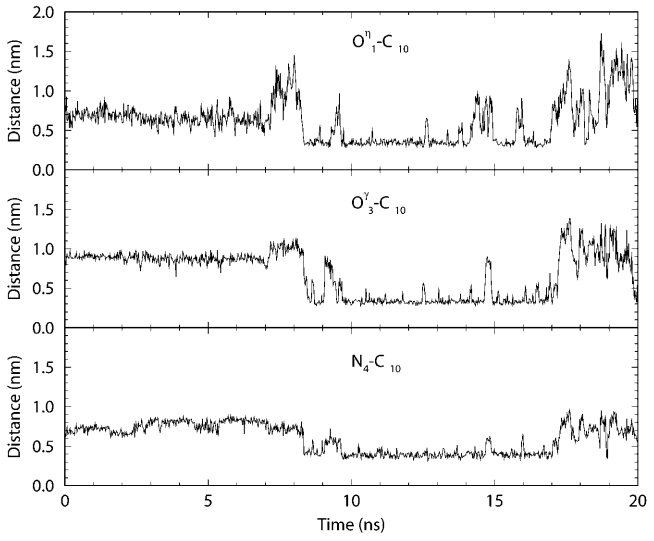

FIGURE 7 The time histories corresponding to the Tyr, Ser, and carboxylate cluster distances observed during the T3S simulation. A stable cluster was observed between 8 and 17 ns.

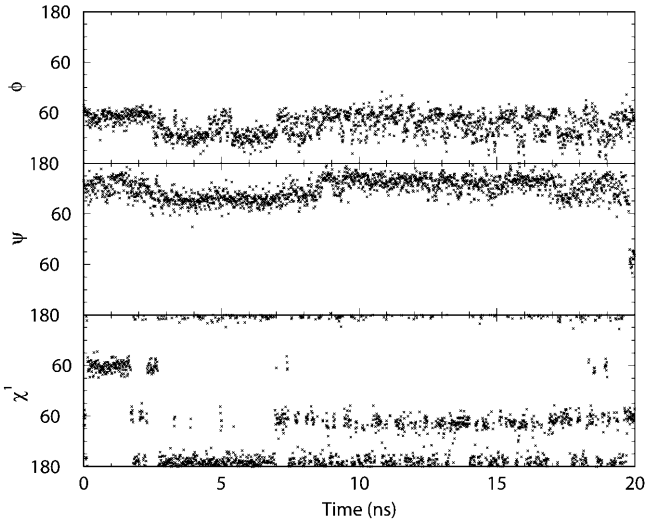

FIGURE 9 Time histories for the φ, ψ, and χ^1 dihedrals of Ser3 obtained from the T3S mutant simulation. During the time the Ser3 cluster was stable (8–17 ns) only g^- and t conformations of χ^1 were observed.

the g^- and t minima of χ^1 were sampled. Hence, it appeared that the intrinsic side-chain distribution for Thr was incompatible with the formation of the cluster. Introduction of a Thr residue, which prefers the g^+ state, would destabilize the cluster causing it to break up with the corresponding loss of free energy associated with cluster formation. Furthermore, the χ^1 of Thr adopts the g^+ conformation in the folded hairpin. Hence, this is incompatible with the preferred side-chain preferences of Ser and could explain the initial instability of the folded structure.

CONCLUSIONS

The results presented here provide a plausible explanation for the large stabilization of the unfolded state in the T3S mutant. The data indicate that residual structure in the unfolded state arises due to specific interactions of Ser3 with other residues, although this is clearly not the only possibility. A complete picture of the relative folding thermodynamics in this system is still not possible as the simulations did not display any reversible folding and therefore further simulation could result in significant changes. However, some consistent major features were the similar free energies in the native state, the fact that the WT and T3S ensembles are quite different due to the large free-energy difference between some of the unfolded states, and the small barrier to unfolding for the T3S mutant. A more accurate representation would require the determination of the free-energy differences between all the most populated conformations in both the WT and T3S ensembles. This is not feasible at present. It seems reasonable that the highly populated unfolded state observed during the T3S simulation should dominate the contribution to the average free-energy change. Hence, the averages presented in Table 2 would probably be biased toward the larger values given more initial structures and additional sampling. In comparison, no major stable unfolded conformations were observed during the WT folding trajectory. Correspondingly, the data suggests that the unfolded WT ensemble is rather random in nature, which is supported by the similarity between the average free-energy change of -3.3 ± 0.2 kJ/mol and the dipeptide result of -2.7 ± 0.5 kJ/mol.

The small free-energy changes associated with the folded state could be related to either the requirement of a g^+ arrangement for Thr χ^1 (see Fig. 5), and/or the loss of a specific side-chain contact in the folded state, which partially offsets the usually favorable (-2.7 kJ/mol) Thr to Ser free-energy difference. The large unfavorable free-energy change observed for the mutation of Ser to Thr in the T3S cluster conformations appeared to be the result of two major effects. One being the difference in the intrinsic free energies of the two residues (2.7 kJ/mol), and the other being the penalty associated with maintaining the Thr χ^1 dihedral in the g^- conformation (4.1 kJ/mol). These penalties make the relative free energy of the cluster conformation comparable to that of the other members of the unfolded WT ensemble. The results suggest that 1), a Thr to Ser mutation may not be as conservative as it first appears; and 2), similar effects may be encountered for other β-branched amino acids. Furthermore, the results illustrate the problems that can be encountered if one focuses solely on changes in the native state.

This project was supported by the National Science Foundation.

REFERENCES

Baldwin, R. L., and G. D. Rose. 1999. Is protein folding hierarchic? I. Local structure and peptide folding. *Trends Biochem. Sci.* 24:26–33.

Bartels, C., and M. Karplus. 1997. Multidimensional adaptive umbrella sampling: application to main chain and side chain peptide conformations. *J. Comput. Chem.* 18:1450–1462.

Berendsen, H. J. C., J. P. Postma, W. F. Van Gunsteren, and J. Hermans. 1981. Interaction models for water in relation to protein hydration. *In* Intermolecular Forces. B. Pullman, editor. D. Reidel Publishing Co., Dordrecht, Netherlands. 331–342.

Beutler, T. C., A. E. Mark, R. C. van Schaik, P. R. Gerber, and W. F. van Gunsteren. 1994. Avoiding singularities and numerical instabilities in free energy calculations based on molecular simulations. *Chem. Phys. Lett.* 222:529–539.

Brooks, III, C. L. 2002. Protein and peptide folding explored with molecular simulations. *Acc. Chem. Res.* 35:447–454.

Creighton, T. E. 1984. Proteins: Structures and Molecular Principles. W. H. Freeman and Company, New York.

Daura, X., B. Jaun, D. Seebach, W. F. van Gunsteren, and A. E. Mark. 1998. Reversible peptide folding in solution by molecular dynamics simulation. *J. Mol. Biol.* 280:925–932.

Daura, X., K. Gademann, H. Schafer, B. Jaun, D. Seebach, and W. F. van Gunsteren. 2001. The beta-peptide hairpin in solution: conformational study of a beta-hexapeptide in methanol by NMR spectroscopy and MD simulation. *J. Am. Chem. Soc.* 123:2393–2404.

Daura, X., A. Glattli, P. Gee, C. Peter, and W. F. van Gunsteren. 2002. Unfolded state of peptides. *Adv. Protein Chem.* 62:341–360.

de Alba, E., M. A. Jimenez, and M. Rico. 1997a. Turn residue sequence determines beta-hairpin conformation in designed peptides. *J. Am. Chem. Soc.* 119:175–183.

de Alba, E., M. Rico, and M. A. Jimenez. 1997b. Cross-strand side-chain interactions versus turn conformation in beta-hairpins. *Protein Sci.* 6: 2548–2560.

de Alba, E., M. Rico, and M. A. Jimenez. 1999. The turn sequence directs beta-strand alignment in designed beta-hairpins. *Protein Sci.* 8:2234–2244.

Dill, K. A., and D. Shortle. 1991. Denatured states of proteins. *Annu. Rev. Biochem.* 60:795–825.

Ferrara, P., J. Apostolakis, and A. Caflisch. 2002. Evaluation of a fast implicit solvent model for molecular dynamics simulations. *Proteins.* 46:24–33.

Fersht, A. R., and V. Daggett. 2002. Protein folding and unfolding at atomic resolution. *Cell.* 108:573–582.

Griffiths-Jones, S. R., A. J. Maynard, and M. S. Searle. 1999. Dissecting the stability of a beta-hairpin peptide that folds in water: NMR and molecular dynamics analysis of the beta-turn and beta-strand contributions to folding. *J. Mol. Biol.* 292:1051–1069.

Hammack, B. N., C. R. Smith, and B. E. Bowler. 2001. Denatured state thermodynamics: residual structure, chain stiffness and scaling factors. *J. Mol. Biol.* 311:1091–1104.

Hennig, M., W. Bermel, A. Spencer, C. M. Dobson, L. J. Smith, and H. Schwalbe. 1999. Side-chain conformations in an unfolded protein: χ^1 distributions in denatured hen lysozyme determined by heteronuclear 13C, 15N NMR spectroscopy. *J. Mol. Biol.* 288:705–723.

Hu, H., M. Elstner, and J. Hermans. 2003. Comparison of a QM/MM force field and molecular mechanics force fields in simulations of alanine and glycine ''dipeptides'' (Ace-Ala-NME and Ace-Gly-NME) in water in relation to the problem of modeling the unfolded peptide backbone in solution. *Proteins.* 50:451–463.

Klimov, D. K., D. Newfield, and D. Thirumalai. 2002. Simulations of beta-hairpin folding confined to spherical pores using distributed computing. *Proc. Natl. Acad. Sci. USA.* 99:8019–8024.

Kollman, P. 1993. Free energy calculations: applications to chemical and biochemical phenomena. *Chem. Rev.* 93:2395–2417.

Kumar, S., D. Bouzida, R. H. Swendsen, P. Kollman, and J. M. Rosenberg. 1992. The weighted histogram analysis method for free-energy calculations on biomolecules. I. The method. *J. Comput. Chem.* 13: 1011–1021.

Ma, B., and R. Nussinov. 2000. Molecular dynamics simulations of beta-hairpin fragment of protein G: Balance between side-chain and backbone forces. *J. Mol. Biol.* 296:1091–1104.

Makarov, V. A., B. K. Andrews, and B. M. Pettitt. 1998. Reconstructing the protein-water interface. *Biopolymers.* 45:469–478.

McCammon, J. A., and S. C. Harvey. 1988. Dynamics of Proteins and Nucleic Acids. Cambridge University Press, Cambridge, MA.

Mitsutake, A., Y. Sugita, and Y. Okamoto. 2001. Generalized-ensemble algorithms for molecular simulations of biopolymers. *Biopolymers.* 60:96–123.

Munoz, V., P. A. Thompson, J. Hofrichter, and W. A. Eaton. 1997. Folding dynamics and mechanism of beta-hairpin formation. *Nature.* 390:196–199.

O'Connell, T. M., L. Wang, A. Tropsha, and J. Hermans. 1999. The ''random-coil'' state of proteins: comparison of database statistics and molecular simulations. *Proteins.* 36:407–418.

Ramirez-Alvarado, M., F. J. Blanco, and L. Serrano. 1996. De novo design and structural analysis of a model beta-hairpin peptide system. *Nat. Struct. Biol.* 3:604–612.

Ramirez-Alvarado, M., F. J. Blanco, and L. Serrano. 2001. Elongation of the BH8 beta-hairpin peptide: electrostatic interactions in beta-hairpin formation and stability. *Protein Sci.* 10:1381–1392.

Ryckaert, J. P., G. Ciccotti, and H. J. C. Berendsen. 1977. Numerical integration of the Cartesian equations of motion of a system with constraints: molecular dynamics of n-alkanes. *J Comput. Phys.* 23:327–341.

Santiveri, C. M., M. Rico, and M. A. Jimenez. 2000. Position effect of cross-strand side-chain interactions on beta-hairpin formation. *Protein Sci.* 9:2151–2160.

Schaefer, M., C. Bartels, and M. Karplus. 1998. Solution conformations and thermodynamics of structured peptides: molecular dynamics simulation with an implicit solvation model. *J. Mol. Biol.* 284:835–848.

Scott, W., P. H. Hunenberger, I. G. Tironi, A. E. Mark, S. R. Billeter, J. Fennen, A. E. Torda, T. Huber, P. Kruger, and W. F. van Gunsteren. 1999. The GROMOS biomolecular simulation program package. *J. Phys. Chem.* 103:3596–3607.

Shortle, D. 1993. Denatured states of proteins and their roles in folding and stability. *Curr. Biol.* 3:66–74.

Smith, P. E., and W. F. van Gunsteren. 1994. Consistent dielectric properties of the simple point charge and extended simple point charge water models at 277 and 300 K. *J. Chem. Phys.* 100:3169–3174.

Stapley, B. J., and A. J. Doig. 1997. Free energies of amino acid side-chain rotamers in alpha-helices, beta-sheets and alpha-helix N-caps. *J. Mol. Biol.* 272:456–464.

Straatsma, T. P., and J. A. McCammon. 1989. Treatment of rotational isomers in free energy evaluations. Analysis of the evaluation of free energy differences by molecular dynamics simulations of systems with rotational isomeric states. *J. Chem. Phys.* 90:3300–3304.

Syud, F. A., H. E. Stanger, and S. H. Gellman. 2001. Interstrand side chain-side chain interaction in a designed beta-hairpin: significance of both lateral and diagonal pairings. *J. Am. Chem. Soc.* 123:8667–8677.

Tironi, I. G., R. Sperb, P. E. Smith, and W. F. van Gunsteren. 1995. A generalized reaction field method for molecular dynamics simulations. *J. Chem. Phys.* 102:5451–5459.

van Gunsteren, W. F., and H. J. C. Berendsen. 1990. Computer simulations of molecular dynamics: methodology, applications and perspectives in chemistry. *Angew. Chem. Int. Ed. Engl.* 29:992–1023.

Wilson, G., L. Hecht, and L. D. Barron. 1996. Residual structure in unfolded proteins revealed by Raman optical activity. *Biochemistry.* 35:12518–12525.

Zerella, R., P. Y. Chen, P. A. Evans, A. Raine, and D. H. Williams. 2000. Structural characterization of a mutant peptide derived from ubiquitin: Implications for protein folding. *Protein Sci.* 9:2142–2150.

Zhou, R., B. J. Berne, and R. Germain. 2001. The free energy landscape for beta hairpin folding in explicit water. *Proc. Natl. Acad. Sci. USA.* 98: 14931–14936.

Zwanzig, R. W. 1954. High-temperature equation of state by a perturbation method. I. Nonpolar gases. *J. Chem. Phys.* 22:1420–1426.